Magnetic fields produced by non-concentric and non-coplanar currents in circular loops

Magnetic fields produced by non-concentric and non-coplanar currents in circular loops

R. Espejel-Morales, G. Murguía-Romero, and A. Calles

Departamento de Física, Facultad de Ciencias, Universidad Nacional Autónoma de México

J.L. Morán-López

División de Materiales Avanzados, Instituto Potosino de Investigación Científica y Tecnológica, San Luis Potosí, México

August 29, 2018

Abstract

A numerical calculation for the stationary magnetic field produced by arrangements of non-concentric and non-coplanar loop current circuits is presented. The calculation is done by superposing the solution of the magnetic field produced by a set of loops with constant currents that mimic two and three dimensional systems. In the three dimensional cases, this is achieved by rotating the magnetic field produced by the non-coplanar loops and adding all the contributions at any arbitrary point in the space. We report the case of two coplanar non-concentric loops that do not overlap and two concentric coplanar rings with different radii carrying currents in the same and opposite directions. Then we consider two non-coplanar rings that are tilted by an angle. More complicated systems consist of a set of loops forming a semi-doughnut. As an extension, we add at the two ends of this system concentric loops to form a horseshoe magnet with a circular cross-section and analyze the results as a function of its geometric characteristics. We can calculate the solutions of the magnetic field in all the space and plot their field lines using a technique that makes use of the Runge-Kutta fourth-order method. In all the cases we plot with different colors the field lines to give information on their strength.

Keywords: Magnetic field; non-concentric loops; numerical calculation of non-concentric current loops.

Introduction

In a recent publication, we reported the calculation of the magnetic fields produced by homogeneously charged objects with axial symmetry, rotating along their symmetry axis [1]. We took advantage of the superposition principle to calculate the magnetic field produced by the objects, assuming that they are made of a set of circular loops. We superposed the analytic solution of all the loops to obtain the magnetic field in all the space. Furthermore, in all the examples some of the magnetic field lines were drawn using a numerical Runge-Kutta fourth order method [2].

The cases reported were a rotating disk; a hollow sphere, where the internal magnetic field is strictly homogeneous; ellipsoids with various eccentricities; cylinders, capped and uncapped in which we combine the solution of a hollow cylinder with one disk at one end or capped at both ends; and an object composed by two spheres and a cylinder. Similar problems have been the subject of various recent publications [3, 4, 5].

All the cases mentioned have azimuthal symmetry and the problem reduces to sum the contribution of concentric loops with particular radii and electric currents. In this paper, we go a step further and use the superposition principle to calculate the magnetic field produced by a set of circular current loops that are non-concentric and/or non-coplanar. The simplest examples consist of two non-overlapping loops on the same plane with the same radii and two concentric coplanar circuits with different radii, in both cases we assume that the loops carry equal currents flowing in the same or opposite directions as shown in figures 1 and 2. Then, we present the case of loops with the same radii but tilted an angle η one with respect to the other and being part of a doughnut. To calculate the magnetic fields in this example, we calculate the magnetic field of one loop, rotate the vector field $\vec{B}$ by an angle η and sum the contributions of one loop on the xy-plane and the other that is tilted. As pointed out in a publication at the beginning of this millennium, Grivich and Jackson [6] noticed that to rotate a vector field one must apply a vector field operator, which transforms vector fields the way a rotation matrix transforms scalar fields. They applied this operation to calculate the magnetic field produced by a current flowing along a regular n-sided polygon.

We also discuss the case of rings forming a half-doughnut, i.e. a set of n loops tilted by an angle π/n following that geometry. Finally a horseshoe magnet is modeled by a set of circular loops added to the two ends of the half-doughnut. In all the cases, we calculate the magnetic field along particular directions and plot the magnetic field lines using the Runge-Kutta method; we plot the lines with different colors to give an idea of the magnetic field strength.

For completeness, in section 1 we recall the well known calculation of the magnetic field produced by a single loop with radius a, that carries a stationary current I. In section 2 we present the case of two coplanar non-concentric and non-overlapping loops with the same radii and carring stationary currents of the same magnitude I, flowing in the same and opposite directions. In section 3 we analyze the rotation of a vector field, and we study the magnetic fields produced by various arrangements that are part of a cylindrical cross-section horseshoe; first we study two loops whose planes are tilted by an angle $\eta = \pi/4$ and their centers are in a circle of radius $2a$. Next we consider a set of five loops that form a half doughnut and finally we add pairs of loops to model the horseshoe with circular cross section. Finally, in section 4 we present our conclusions.

1 The magnetic field produced by a current in a circular loop

Since all our discussion and results are based on the magnetic field of a circular loop carrying an stationary electric current I, throughout the discussion we will use cylindrical coordinates (ρ, z, ϕ).

As it is well known, the magnetic field produced at any point of the space, $\vec{r}(\rho, z)$, by a circular loop of an infinitely thin wire located at the xy plane, with radius a, centered in the origin and in which an stationary electric current I is flowing, is independent of ϕ and the polar components of the $\vec{B}$ field are given by the following equations [7]:

$$B_\rho = B_0 \frac{\gamma}{\pi\sqrt{\delta}} \left[\frac{1+\alpha^2+\beta^2}{\delta - 4\alpha^2} E(k^2) - K(k^2) \right] , \tag{1}$$

$$B_z = B_0 \frac{\gamma}{\pi\sqrt{\delta}} \left[\frac{1-\alpha^2-\beta^2}{\delta - 4\alpha^2} E(k^2) - K(k^2) \right] , \tag{2}$$

where,

$$\alpha = \frac{\rho}{a} \, , \beta = \frac{z}{a} \, , \gamma = \frac{z}{\rho} \, , B_0 = \frac{\mu_0 I}{2a} \, , \delta = (1+\alpha)^2 + \beta^2 \, , k^2 = \frac{4\alpha}{\delta} \, . \tag{3}$$

K and E are the complete elliptic integrals of first and second kind, respectively.

Equation (2) could be written as the well known expression:

$$B_z = \frac{\mu_0 I a^2}{2(a^2+z^2)^{3/2}} \ . \tag{4}$$

Notice that the magnetic filed lines can be characterized by

$$\frac{d\vec{r}}{ds} = \hat{B}(\vec{r}) \ , \tag{5}$$

where ds is a differential distance along the line and $\hat{B}(\vec{r})$ is a unit vector along the field. Equation (5) can be expressed in terms of the polar components, as

$$\frac{d\rho}{ds} = \frac{B_\rho}{B}, \quad \rho\frac{d\phi}{ds} = \frac{B_\phi}{B}, \quad \frac{dz}{ds} = \frac{B_z}{B} \ , \tag{6}$$

where B_ρ, B_ϕ and B_z are the cylindrical components of the magnetic field. Equation (6) gives place to an ordinary differential coupled equations. To solve it, we make use of the fourth order Runge-Kutta method. Its solution defines the field line curves in three-dimensional space. For more details the reader is referred to Ref. 1.

2 The magnetic field of two coplanar non-concentric loops

In this section we calculate the magnetic field produced by two non-concentric coplanar loops with radius a, carrying an stationary current I in both, the same and opposite directions. The two loops are on the xy-plane, the origin of the coordinate system is located at the center of the left-hand loop and the center of the second loop we choose it at $(0, 4a, 0)$.

The magnetic field produced by the first loop is given by equations 1 to 3. The second one is obtained by translating the center of the loop to $(0, 4a, 0)$. The total field in each point of the space, is simply the superposition of the contributions of both magnetic fields. Figure 1(a) shows the field lines on the yz-plane produced by the two loops carrying a current in the same direction. In this case, the magnetic field along the line perpendicular to the y-axis that crosses at $y = 2a$, $\vec{B}_z(0, 2a, z)$, is parallel to the z-axis and different from zero everywhere, except for two symmetric points above and below the y-axis. At those points the magnetic field produced by both rings cancels each other, this means $B_x(0, 2a, z) = 0$ and $B_y(0, 2a, z) = 0$.

Figure 1(c) shows the dependence of $B_z(0, y, 0)$ as a function of y for the range $-2a \leq y \leq 6a$. In this case, for large negative values the field is small and negative. As the y values reach the ring border, the field increases and diverges at $y = -a$. For values inside the ring, B_z acquires large positive values and decreases to the value close to $B_z = B_0 = \mu_0 I/2a$. The discontinuities at the ring boundaries, arise from the $1/r$ dependence of the magnetic field produced by a linear wire. From one side of the ring it is positive, and negative from the other side. In the space between the rings, apart from the edge discontinuities, the magnetic field is small and almost uniform for a long range with a minimum value at $y = 2a$. The magnetic field for values $y > 2a$ has the same characteristics to the one described for the left ring.

It is worth mentioning that the diverging form of B_z shown in the figures 1(c) and 2(c), is physically meaningless due to the fact that the solution is valid only far enough from a real current carrying wire.

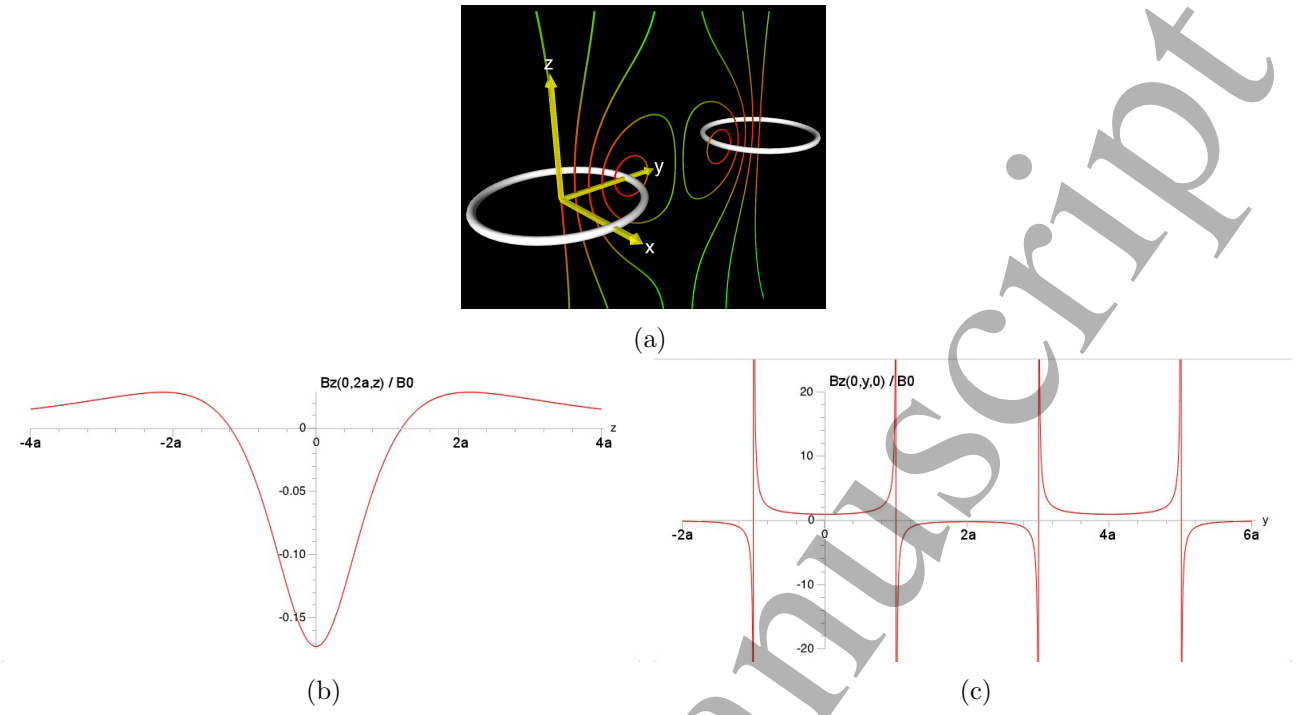

Figure 1: (a) Some of the field lines on the yz-plane, produced by two non-concentric coplanar loops with the same radii a, carrying a stationary current I in the same direction. The strength of the magnetic field is denoted by a different color, being red (green) the most (less) intense. (b) The dependence of z-component of the magnetic field as a function of z for the range $-4a \leq z \leq 4a$. The z-values were taken along the line perpendicular to the y-axis that crosses at $y = 2a$. (c) The dependence of $B_z(0, y, 0)$ as a function of y for the range $-2a \leq y \leq 6a$. The center of the loops are located at $y = 0$ an $y = 4a$.

The magnetic field lines for the case in which the currents of the two rings flow in opposite directions is shown in figure 2(a). Comparing these field lines with those of figure 1(a), the difference between both cases is clear. In the case of opposite current flows, $B_z = 0$ along the whole line $(0, 2a, z)$ but the component B_y along the same line is different from zero except at $z = 0$. The z dependence of the magnetic field is shown in figure 2(b). It has negative values as one approaches the xy-plane from negative z values, acquires its minimum value and then changes its sign at $z = 0$. For positive values of z, the magnetic field increases to a maximum value and then decreases for larger values. In figure 2(c) we show the y dependence of B_z for the same range of y values as figure 1(c). The discontinuities at the rim values are present and follow the direction of the right hand rule. In the point between the two rings the magnetic field vanishes.

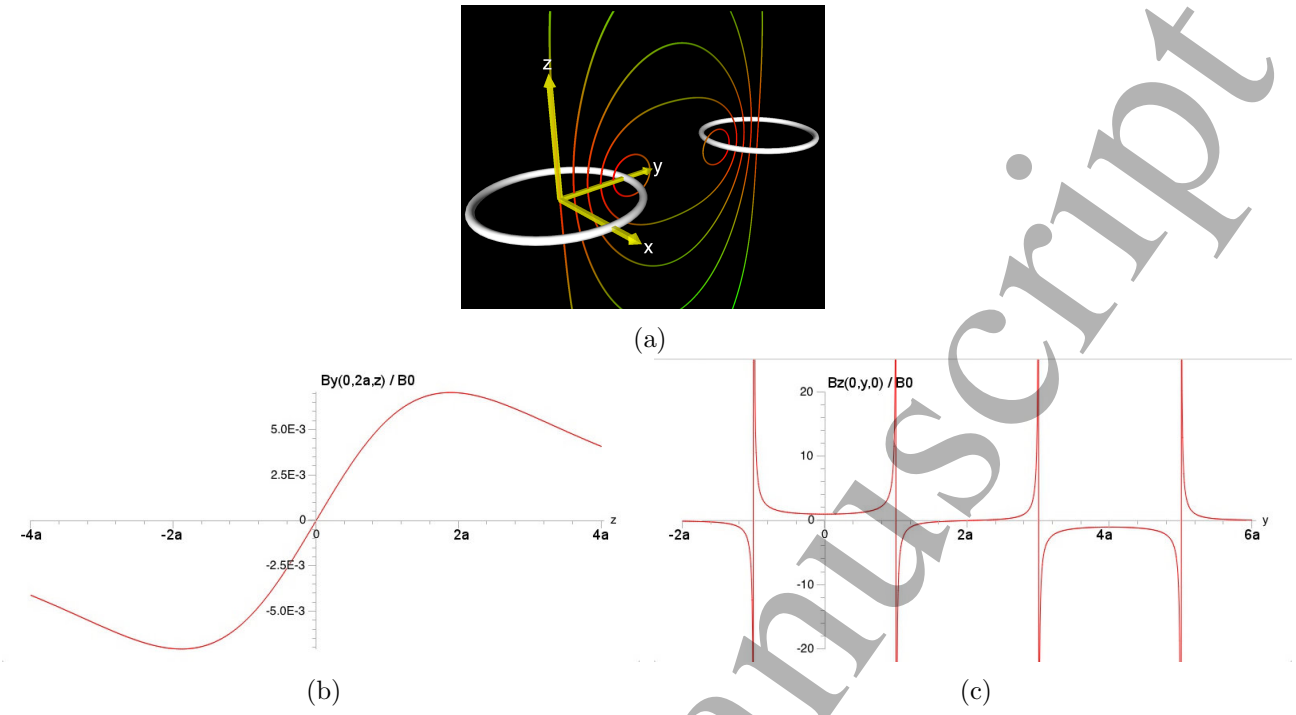

Figure 2: (a) Some of the field lines on the yz-plane, produced by two non-concentric coplanar loops with the same radii a, carrying a stationary current I in opposite directions. The strength of the magnetic field is denoted by a different color, being red (green) the most (less) intense. (b) The dependence of y-component of the magnetic field as a function of z for the range $-4a \leq z \leq 4a$. The z-values were taken along the line perpendicular to the y-axis that crosses at $y = 2a$. (c) The dependence of $B_z(0, y, 0)$, as a function of y for the range $-2a \leq y \leq 6a$.

3 Rotation of vector fields

Here we outline the theory to calculate the magnetic field $\vec{B}$ that is produced by a loop of radius a carrying an stationary current I, which lies on a plane that is tilted an angle θ around the x axis, as illustrated in figure 3(a). The coordinate system in which the loop lies is called $x'y'z'$. The goal is to calculate the magnetic field in the xyz coordinate system.

We proceed as follows: First we rotate the $x'y'z'$ arround the common x and x' direction by an angle $-\theta$, such that the two coordinate systems coincide and the loop is on the xy plane. This means that we rotate the tilted loop to finally set it on the xy-plane (figure 3(b)). The relationship between the tilted coordinates and the original ones are given by

$$\begin{aligned} x' &= x, \\ y' &= y\cos(\theta) + z\sin(\theta), \\ z' &= z\cos(\theta) - y\sin(\theta). \end{aligned}$$

Now one can calculate the field components (B_x, B_y, B_z) that corresponds to the loop on the plane xy. The component B_z is given by equation (2) and the components B_x and B_y are given in terms of B_ρ by

$$\begin{aligned} B_x &= B_\rho \sin(\phi), \\ B_y &= B_\rho \cos(\phi), \end{aligned}$$

with $\phi = \arctan(y/x)$.

Thus, the magnetic field $\vec{B}'$ in the original system produced by the tilted loop (figure 3(c)), can be obtained by performing an inverse rotation of the field components (B_x, B_y, B_z) through the next transformations:

$$
\begin{aligned}
B'_x(x,y,z) &= B_x(x',y',z') \\
B'_y(x,y,z) &= B_y(x',y',z')\cos(\theta) - B_z(x',y',z')\sin(\theta), \\
B'_z(x,y,z) &= B_y(x',y',z\prime)\sin(\theta) + B_z(x',y',z')\cos(\theta),
\end{aligned}
$$

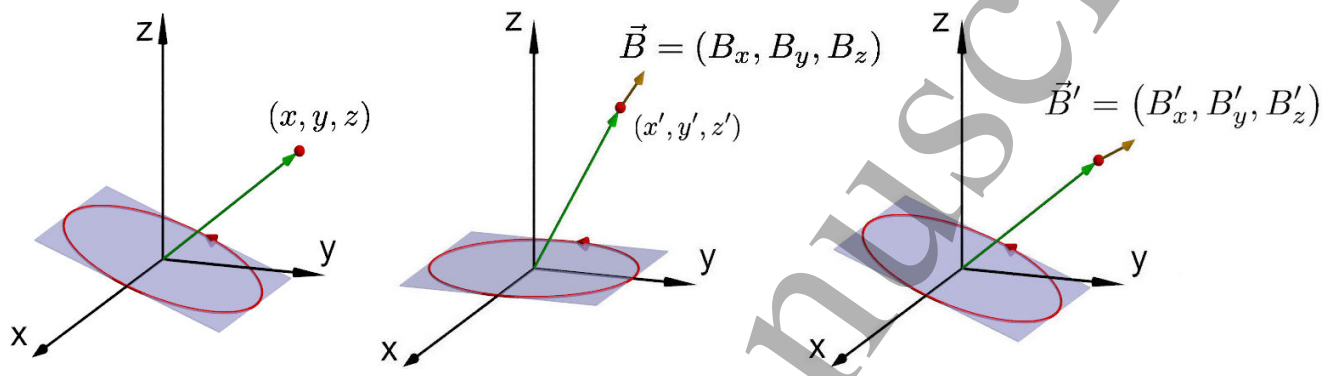

(a) (b) (c)

Figure 3: Procedure to calculate the magnetic field $\vec{B}$ that is produced by a loop which is tilted an angle θ around the x axis (a). The system is tilted by an angle $-\theta$ and the field components (B_x, B_y, B_z), that corresponds to the loop on the plane xy, are calculated (b). Finally, the magnetic field in the original system, produced by the tilted loop, can be obtained by performing an inverse rotation of the field components (c).

Finally, by using the superposition principle, we can calculate the magnetic filed of systems made of two non-coplanar rings, as one lying on the xy-plane and the other, tilted by an angle θ around the x axis.

3.1 Two non-coplanar and non-concentric rings

We now apply the theory to two non-coplanar and non-concentric circular loops with radii a and carrying an stationary current I in the same direction. These two rings follow the geometry of a doughnut; i.e. the centers of the two rings lie on the internal circle of the doughnut. We choose $\theta = \pi/4$ for the angle between the two ring planes.

In figure 4 we show some magnetic field lines and the magnetic dipole at the center of each loop. If the field line is close to one of the rings and in the space where the two rings are far apart, they follow the normal circular path along the ring (path a). If the line is close to the region where the two rings are close, the magnetic fields produced by the two conductors add to generate a path that is a distorted circle (path c). For regions that are not to close to the rings and where they are more separated, the field line follows a complicated path in the form of a number eight in which the extreme parts follow a semicircle (paths b).

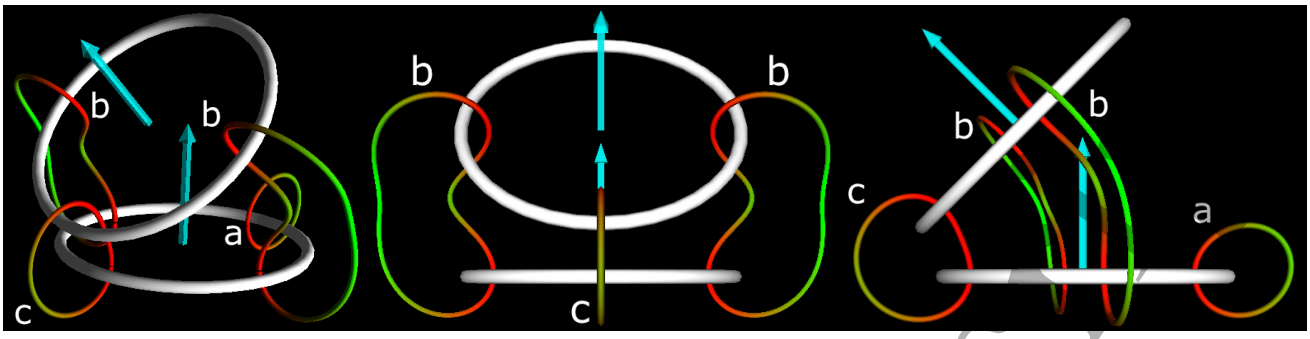

Figure 4: Some magnetic field lines produced by two non-coplanar and non-concentric circular loops carrying a current in the same direction. The centers of the two rings lie on a circle. The angle between the two ring planes is $\pi/4$. The blue arrows denote the magnetic moment of each loop.

3.2 A semi-doughnut system

We model now a semi-doughnut with five circular rings arranged in a geometry such that the centers of the rings are located along a half a circle corresponding to the internal center of a doughnut. The angle between each pair of neighbor planes containing the rings is, obviously, $\pi/4$; in this way we complete a semi-doughnut with five rings.

The figures 5(a), 5(b) and 5(c) we show some of the magnetic field lines seen from different perspectives. In figure 5(a) the central ring lies in the plane perpendicular to the paper sheet and the field lines that go through this ring are symmetric to it. Note that the different field strengths are shown with different colors (red is intense and green is weak). As expected, the field strength is reduced as one moves close to the most external part of the doughnut. We also show two field lines that pass only through the two extreme rings. Viewing the system with the central loop lying on the plane of the view, we obtain the figure 5(b). The field lines that cross the central ring are also symmetric. In figure 5(c) we show several field lines that pass along the diameter of the central ring. This case corresponds to a view of the system rotated along the z-axis by $\pi/4$. Here we also observe the obvious reduction of the magnetic field strength as the lines go into the open space.

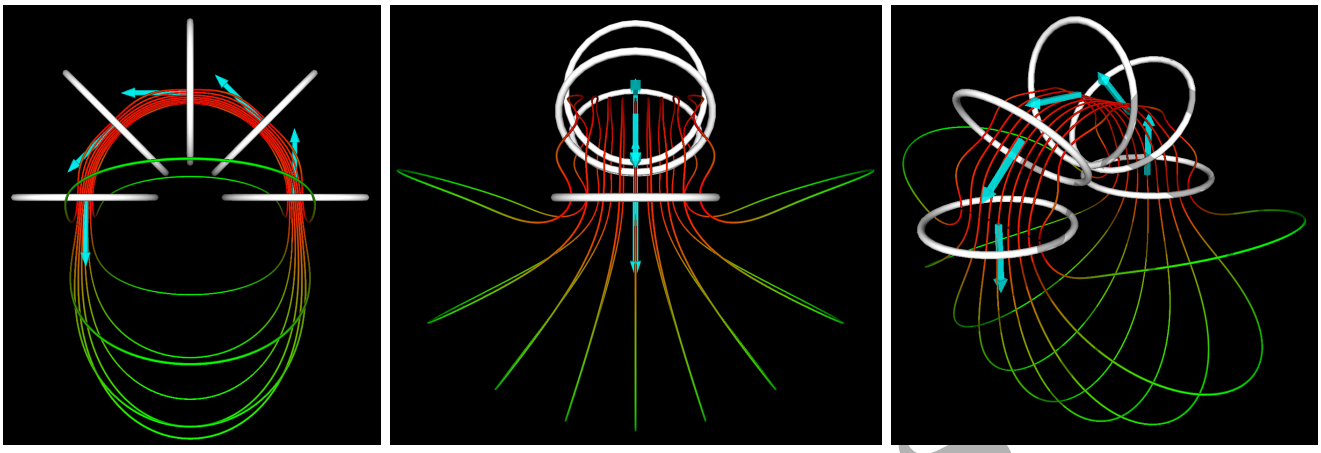

(a) (b) (c)

Figure 5: Some of the magnetic field lines (seen from different perspectives) produced by five circular loops with the same radii a, carrying the same current I whose centers lie in a circle. The angle between each pair of neighbor planes containing the rings is $\pi/4$. The blue arrows denote the magnetic moment of each loop.

3.3 A horseshoe system

We now proceed to model a horseshoe magnet. We take the semi-doughnut discussed above and add to the extremes two rings along the z-axis equally spaced by a distance $a/2$. Thus we have a horseshoe with cylindrical legs. All the rings have the same radii a and carry an stationary current I.

The results for the magnetic field lines that pass through the horizontal diameter line of the top ring are shown in figures 6(a), 6(b) and 6(c). Figure 6(a) shows the results as seen from a frontal view. A side view is presented in figure 6(b), where it can be seen how some lines at the extremes extend out of the horse shoe body. In figure 6(c) we show the field lines from a rotated perspective that shows more clearly the geometry of the field lines.

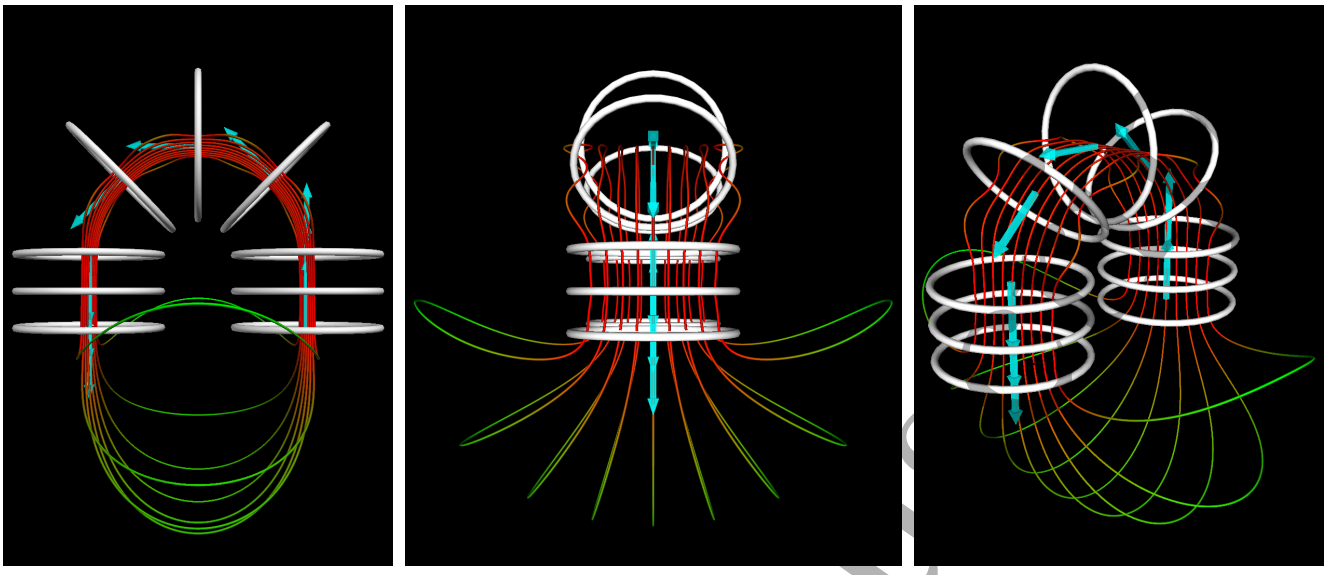

(a) (b) (c)

Figure 6: Some of the magnetic field lines (seen from different perspectives) produced by a model of a horseshoe magnet formed by a semi-doughnut and two rings added to the extremes along the z-axis equally spaced. All the rings have the same radii a and carry the same current I. The blue arrows denote the magnetic moments associate to each ring. The blue arrows denote the magnetic moment of each loop.

3.3.1 Horseshoe system analysis

Notice that there is a dependence between the number of pairs of rings added to the semi-doughnut to form the horseshoe and the shape of the field lines. In particular, the field lines close to the inner border of the last ring bend outwards at different angles. To show this effect, the field line that passes through the points with coordinates $(0.8a, 0, z_e)$ was calculated, where z_e is the z-coordinate of the lowest ring. We call P_1 and P_2 the points of the field line (symmetrical with respect to the xz plane) for which the radius of curvature is minimal (green dots in Fig. 7(a)). Observe that a plane can be defined using P_1, P_2 and the point in the field line that is furthest away from the yz plane, P_3 (red dot). Furthermore, it is worth noticing that the horseshoe plane of symmetry is the plane yz and the first loops that complete the semi-doughnut are in the xy-plane. The angle between the xy-plane and that defined by P_1, P_2 and P_3 is denoted by θ.

We estimated the angle between those planes as a function of the number of pair of rings n added to the semi-doughnut. The space between neighbor pairs is $a/2$ and $n = 0, 1, \ldots, 16$.

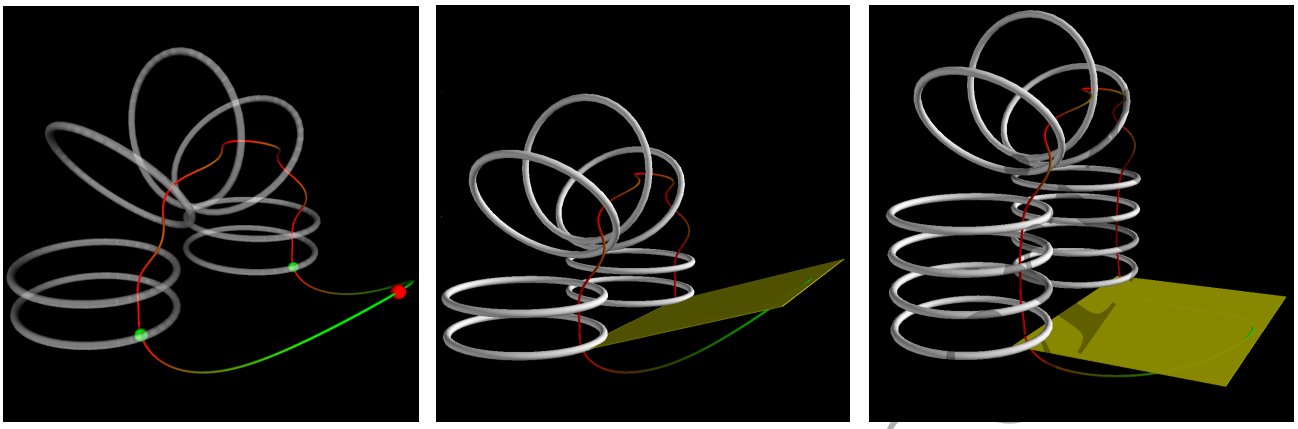

(a) (b) (c)

Figure 7: Figure (a) shows the positions of the points P_1, P_2 and P_3 (see text), the rings have been drawn transparent. In Figures (b) and (c) the examples for $n = 1$ and $n = 3$, respectively.

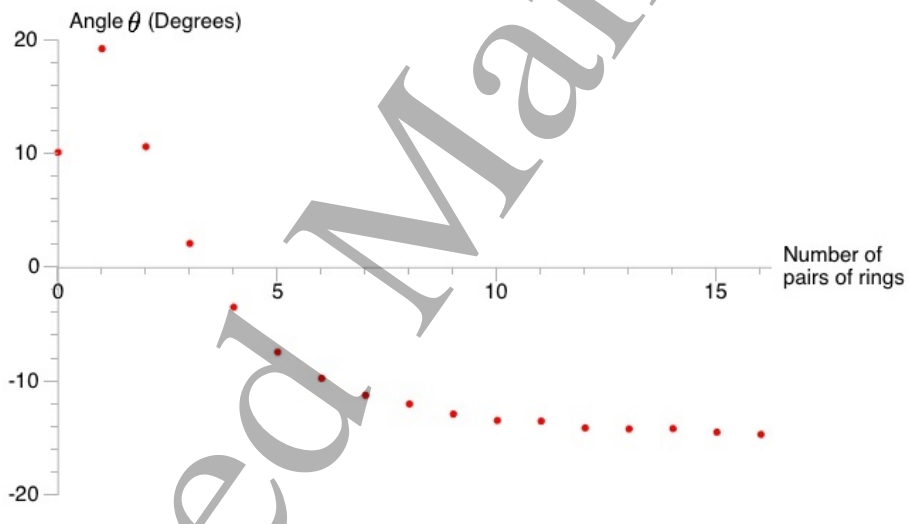

Figure 8: The dependence of θ on n; the angle between the plane defined by P_1, P_2 and P_3, and the xy-plane for a horseshoe magnet with legs formed by n pairs of rings added to the semi-doughnut.

In Figures 7(b) and 7(c) we show the plane for $n = 1$ and $n = 3$, respectively. The plane for $n = 3$ is almost parallel to the xy-plane. The dependence on n of θ is presented in Figure 8. Observe that the angle θ goes from positive to negative values and tends very rapidly to an asymptotic value as a function of the length of the horseshoe legs.

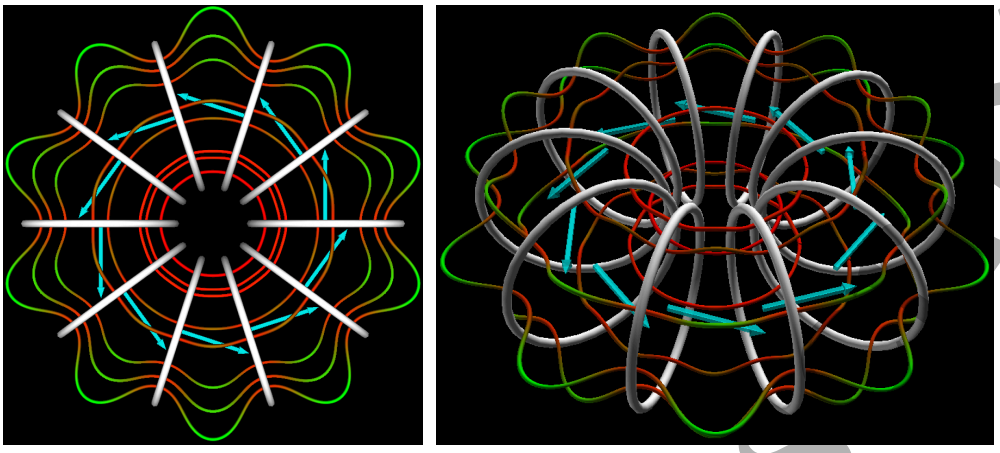

(a) (b)

Figure 9: Some of the magnetic field lines (seen from different perspectives) produced by ten circular rings with the same radii a, carrying the same current I, forming a doughnut. The centers of the loops are located along a circle. The angle between each pair of neighbor planes containing the rings is $\pi/5$. The blue arrows denote the magnetic moment of each loop.

3.4 A doughnut system

The next example corresponds to a doughnut. We construct the system with ten rings, the angle between two consecutive rings is $\pi/5$. All the rings are equivalent and carry an stationary current I in the same direction.

In figure 9(a) we show some field lines from a top view. All the field lines shown are trapped inside the doughnut and the strength of the magnetic field diminish as one moves to the external part. The blue arrows denote the dipole moments of each ring. The most external field lines are wavy curves that extend outside the doughnut space. This effect is reduced as the number of rings in the system increases. Figure 9(b) shows the field lines from a non-symmetric perspective presenting the rich geometrical characteristics of the field lines, including the ten-fold symmetry.

4 Conclusions

We have presented a method that allows to obtain the magnetic field produced by non-concentric and non-coplanar circular loops carrying constant current. For simplicity we assumed, in all the examples, circular loops with the same radii and carrying the same intensity of the current.Nevertheless, this method can be applied to any circular loop geometries and parameters by making use of the superposition principle and performing the necessary tilts of the loops composing the system. In all the cases presented in this paper, we calculated the magnetic field and, using the four order Runge-Kutta method, we draw some of the field lines to show their complexity and beautiful geometry.

The examples presented here, help the reader to visualize and appreciate the magnetic field produced by stationary currents flowing in arbitrary space arrangements of any number of tilted circular loops. Furthermore, this work could help to enhance the teaching of vectorial transformations in combination with the superposition principle in magnetic field calculations at both undergraduate and early graduate level. In addition, the implementation of numerical methods to visualize the field lines, would allow them to solve more complex examples than those presented in the textbooks.

Systems consisting of any number of tilted loops and arbitrary oriented linear wires can be also studied by this method. It is to foresee an even more interesting magnetic behavior for these cases.

Acknowledgements

This work has been supported by DGTIC-UNAM, with the access to the 375 Miztli-UNAM supercomputer, with the project LANCAD-UNAM-DGTIC-055. The authors acknowledge support from DGAPA-UNAM grand under PAPIIT IN114318 and PAPIME PE101015 projects.

References

[1] Espejel-Morales R, Murguía-Romero G, Calles A, Cabrera-Bravo E and Morán-López J L 2016 *Eur. J. Phys.* **37** 045204

[2] Mathews J H and Fink K K 1999 *Numerical Methods Using Matlab* 3rd edn (Englewood Cliffs, NJ,; Prentice Hall) p 460

[3] Avila M A 2003 *Rev. Mex. Fis.*, **49** 182

[4] Camacho J M and Sosa V 2013 *Rev. Mex. Fis. E* **59** 8-17

[5] Wan S, Teng B, Chen X, Fu H, Li Y, Wu M, and Balfour E A 2014 *Eur. J. Phys.* **35** 035005

[6] Grivich M I and Jackson D P 2000 *Am. J. Phys.* **68** 469-74

[7] Smythe W R 1959 *Static and Dynamic Electricity* (New York: McGraw-Hill) p 290

[8] Griffiths D J 1989 *Introduction to electrodynamics*, 2nd Edition (Prentice Hall), New Jersey 236-7

[9] Purcell E M and Morin D J 2013 *Electricity and Magnetism*, 3rd Edition (Cambridge University Press) pp 299-302